

# Adjoint and direct characteristic equations for two-dimensional compressible Euler flows.

Kevin Ancourt<sup>a</sup>, Jacques Peter<sup>\*a</sup>, Olivier Atinault<sup>b</sup>

<sup>a</sup>*Département aérodynamique, aéroélasticité et acoustique (DAAA), ONERA, Université Paris Saclay, 29 avenue de la Division Leclerc, Châtillon, 92322, France*

<sup>b</sup>*Département aérodynamique, aéroélasticité et acoustique (DAAA), ONERA, Université Paris Saclay, 8 Rue des Vertugadins, Meudon, 92190, France*

---

## Abstract

The method of characteristics is a classical method for gaining understanding in the solution of a partial differential equation. It has recently been applied to the adjoint equations of the 2D Euler equations and the first goal of this paper is to present a linear algebra analysis that greatly simplifies the discussion of the number of independent characteristic equations satisfied along a family of characteristic curves. This method may be applied for both the direct and the adjoint problem and our second goal is to directly derive in conservative variables the characteristic equations of 2D compressible inviscid flows. Finally, the theoretical results are assessed for a nozzle flow with a classical scheme and its dual consistent discrete adjoint.

*Key words:* Continuous adjoint, inviscid flow, compressible flow, method of characteristics, characteristic equation, characteristic curve

---

## 1. Introduction

The method of characteristics is a well-known method for studying partial differential equations (PDE). It aims to exhibit specific hypersurfaces in the input domain where the solution of the PDE of interest satisfies an ordinary differential equation (ODE). When applied to 2D inviscid compressible flows, it is known to provide a full resolution of a supersonic area only based on the knowledge of the inflow (whereas it provides partial information for a subsonic flow) [1, 2, 3, 4]. Both theoretical understanding and practical calculations of a variety of flows (in nozzles, along steps, along curved walls) are enabled by this technique.

Besides, discrete and continuous adjoint are now well-established methods for shape optimization [5, 6, 7, 8, 9] and goal-oriented mesh adaptation [10, 11, 12]. Because of these important applications, regular efforts have been devoted to the fast and safe writing of adjoint modules [13, 14, 15, 16] and to the efficient solving of the adjoint equations [17, 18]. Adjoint methods are also useful for flow control [19, 20], meta-modelling [21, 22], receptivity-sensitivity-stability analyses [23, 24], data assimilation [25, 26]. In a recent paper [27] the characteristic equations (CE) for the adjoint 2D Euler equations have been derived.

The classical direct characteristic equations (DCE) for 2D inviscid compressible flows and the recently presented corresponding adjoint characteristic equations (ACE) appear to be linked; In particular, the characteristic curves are the same for both problems [27]. The analogies between (ACE) and (DCE) are further studied in section 2 where several properties of a generic system of equations embedding (ACE) and (DCE) are demonstrated. In particular, this formal linear algebra approach greatly simplifies the determination of the number of independent (CE) satisfied along two families of characteristic curves.

Whereas the (ACE) need to be derived from the complete 8x8 linear system for the Cauchy problem – the (DCE) have

---

\*Corresponding author. Tel.: +33 1 46 73 41 84.

*Email addresses:* kevin.ancourt@onera.fr (Kevin Ancourt), jacques.peter@onera.fr (Jacques Peter), olivier.atinault@onera.fr (Olivier Atinault)

been derived with various mechanical assumptions and also various sets of variables. For the sake of a full understanding, the direct characteristic problem is solved in conservative variables from the complete Cauchy problem and the resulting differential forms are discussed in section 3.

Finally, an inviscid supersonic nozzle flow is considered in section 4 where both the (DCE) and the (ACE) are numerically assessed.

## 2. Common properties of the linear systems for the Cauchy direct and adjoint problems

### 2.1. Notations

We denote by  $W = (\rho, \rho u, \rho v, \rho E)$  the conservative variables, with  $\rho$  the density,  $(u, v)$  the components of the velocity  $\bar{U}$ , by  $e$  the internal energy, by  $E$  the total energy. A thermally and calorically perfect gas law is considered. The static pressure  $p$ , total enthalpy  $H$  and entropy  $S$  read

$$p = (\gamma - 1)\rho e = (\gamma - 1)(\rho E - 0.5\rho|\bar{U}|^2)$$

$$H = E + \frac{p}{\rho} \quad S = c_v \ln\left(\frac{p}{\rho^\gamma}\right)$$

with a constant  $\gamma = 1.4$  and a constant heat capacity at constant volume,  $c_v$ . A subscript  $i$  is used to denote the classical stagnation quantities  $(\rho_i, p_i, T_i)$ . Finally, the adjoint vector of the functional output of interest is denoted as  $\Psi = (\psi_1, \psi_2, \psi_3, \psi_4)$ .

### 2.2. Generic Cauchy problem embedding (ACE) and (DCE)

Given  $a$  and  $b$ , two neighboring points in the fluid domain, we denote by  $(dx, dy) = \vec{ab}$ . The increment in the adjoint components between the two points are denoted as  $(d\psi_1, d\psi_2, d\psi_3, d\psi_4) = (\psi_1^b - \psi_1^a, \psi_2^b - \psi_2^a, \psi_3^b - \psi_3^a, \psi_4^b - \psi_4^a)$ . The Cauchy problem for the adjoint vector aims at calculating its derivatives at point  $a$  with first order in space, and the singularities of this problem are at the core of the search of the (CE). The corresponding  $8 \times 8$  linear system associates first-order Taylor expansions and the 2D adjoint Euler equations. It reads

$$\begin{bmatrix} dx & 0 & 0 & 0 & dy & 0 & 0 & 0 \\ 0 & dx & 0 & 0 & 0 & dy & 0 & 0 \\ 0 & 0 & dx & 0 & 0 & 0 & dy & 0 \\ 0 & 0 & 0 & dx & 0 & 0 & 0 & dy \\ & & & & & & & \\ & -A^T & & & -B^T & & & \end{bmatrix} \begin{bmatrix} (\partial\psi_1/\partial x) \\ (\partial\psi_2/\partial x) \\ (\partial\psi_3/\partial x) \\ (\partial\psi_4/\partial x) \\ (\partial\psi_1/\partial y) \\ (\partial\psi_2/\partial y) \\ (\partial\psi_3/\partial y) \\ (\partial\psi_4/\partial y) \end{bmatrix} = \begin{bmatrix} d\psi_1 \\ d\psi_2 \\ d\psi_3 \\ d\psi_4 \\ 0 \\ 0 \\ 0 \\ 0 \end{bmatrix} \quad (1)$$

where  $-A^T$  and  $-B^T$  are the opposite and transposed Jacobians of the Euler fluxes. The straightforward counterpart for the derivatives of the discrete flow field  $W$ , appears in equation (15). Several results regarding the minors of the matrices in (1) and (15) and also the number of independant (CE) when  $(dx, dy)$  make the  $8 \times 8$  matrices singular may be demonstrated considering a generic matrix

$$\mathbf{K} = \begin{bmatrix} dx & 0 & 0 & 0 & dy & 0 & 0 & 0 \\ 0 & dx & 0 & 0 & 0 & dy & 0 & 0 \\ 0 & 0 & dx & 0 & 0 & 0 & dy & 0 \\ 0 & 0 & 0 & dx & 0 & 0 & 0 & dy \\ & & & & & & & \\ & & & & \mathbf{A} & & & \mathbf{B} \end{bmatrix}$$

where  $(\mathbf{A}, \mathbf{B})$  stands either for  $(-A^T, -B^T)$  or for  $(A, B)$ . The corresponding generic notation for  $\psi$  or  $W$  is  $\zeta$ . The columns of  $\mathbf{A}$  and  $\mathbf{B}$  are denoted as  $\{\mathbf{A}_1, \mathbf{A}_2, \mathbf{A}_3, \mathbf{A}_4\}$  and  $\{\mathbf{B}_1, \mathbf{B}_2, \mathbf{B}_3, \mathbf{B}_4\}$ , respectively. We stress that the bold characters are therefore associated with the generic problem and not with a higher tensor order.

### 2.3. Coefficients of (ACE) and (DCE) as $4 \times 4$ determinants

It has already been observed that the direct and adjoint problems share the same determinant, computed using linear combinations of columns, as

$$|\mathbf{K}| = |-dx\mathbf{B} + dy\mathbf{A}| = (-v dx + u dy)^2(-v dx + u dy + c dl)(-v dx + u dy - c dl),$$

with

$$c = \sqrt{\frac{\gamma p}{\rho}}, \quad dl = \sqrt{dx^2 + dy^2},$$

using the known eigenvalues of the Euler flux Jacobian in an arbitrary direction [27]. If  $|\mathbf{K}| \neq 0$ , the Cauchy problem is well-posed, and the solution is expressed using the minors of  $\mathbf{K}$ . These minors are denoted as  $\mathbf{K}_{jx}^i$  and  $\mathbf{K}_{jy}^i$  with indices referring to the considered variable and the direction of differentiation. For example  $(\partial \zeta_1 / \partial x)$  reads

$$\left(\frac{\partial \zeta_1}{\partial x}\right) = \frac{\begin{vmatrix} d\zeta_1 & 0 & 0 & 0 & dy & 0 & 0 & 0 \\ d\zeta_2 & dx & 0 & 0 & 0 & dy & 0 & 0 \\ d\zeta_3 & 0 & dx & 0 & 0 & 0 & dy & 0 \\ d\zeta_4 & 0 & 0 & dx & 0 & 0 & 0 & dy \\ \hline 0 & \mathbf{A}_2 & \mathbf{A}_3 & \mathbf{A}_4 & \mathbf{B}_1 & \mathbf{B}_2 & \mathbf{B}_3 & \mathbf{B}_4 \\ \hline \end{vmatrix}}{|\mathbf{K}|} \quad (2)$$

$$\left(\frac{\partial \zeta_1}{\partial x}\right) = \frac{\mathbf{K}_{1x}^1 d\zeta_1 - \mathbf{K}_{1x}^2 d\zeta_2 + \mathbf{K}_{1x}^3 d\zeta_3 - \mathbf{K}_{1x}^4 d\zeta_4}{|\mathbf{K}|} \quad (3)$$

Conversely, the generic Cauchy problem is ill-posed iff  $|\mathbf{K}| = 0$ , that is along the  $S$ ,  $C^+$  and  $C^-$  curves:

$$-v dx + u dy = 0 \quad S \text{ streamtraces} \quad (\text{all Mach numbers}) \quad (4)$$

$$-v dx + u dy + c dl = 0 \quad C^- \text{ characteristics} \quad (\text{supersonic flow only}) \quad (5)$$

$$-v dx + u dy - c dl = 0 \quad C^+ \text{ characteristics} \quad (\text{supersonic flow only}) \quad (6)$$

In such case, the boundedness of  $(\partial \zeta_j / \partial x)$   $(\partial \zeta_j / \partial y)$  along the characteristic curves and their expression outside these curves yields the (CE). Typically equation (3), that is valid outside the characteristic curves, yields the following (CE)

$$\mathbf{K}_{1x}^1 d\zeta_1 - \mathbf{K}_{1x}^2 d\zeta_2 + \mathbf{K}_{1x}^3 d\zeta_3 - \mathbf{K}_{1x}^4 d\zeta_4 = 0$$

along the characteristic curves. Of course, seven other (CE) are derived from the boundedness of  $(\partial \zeta_2 / \partial x) \dots (\partial \zeta_4 / \partial y)$  and we need to determine a minimal set of independant (CE) for each type of characteristic curve.

To that end, the  $\mathbf{K}_{jx}^i$  and  $\mathbf{K}_{jy}^i$  minors are expressed as determinants of  $4 \times 4$  matrices. From equations (2) and (3),

$$\mathbf{K}_{1x}^1 = \begin{vmatrix} dx & 0 & 0 & 0 & dy & 0 & 0 & 0 \\ 0 & dx & 0 & 0 & 0 & dy & 0 & 0 \\ 0 & 0 & dx & 0 & 0 & 0 & dy & 0 \\ \hline \mathbf{A}_2 & \mathbf{A}_3 & \mathbf{A}_4 & \mathbf{B}_1 & \mathbf{B}_2 & \mathbf{B}_3 & \mathbf{B}_4 & \\ \hline \end{vmatrix}$$

is the basic formula for  $\mathbf{K}_{1x}^1$ . In all 32 corresponding expressions, the  $dy$  terms of the first three lines are eliminated by linear combinations of columns and the determinants are then expanded along these lines.<sup>1</sup> The minors arising in

<sup>1</sup>We assume that  $dx \neq 0$  introducing  $t = dy/dx$  and will further consider this hypothesis in the following. For the sake of brevety we shall not discuss the simple specific case where  $dx = 0$ .

the (CE) derived from the existence of  $(\partial\zeta_1/\partial x)$  then read

$$\begin{array}{llll} \mathbf{K}_{1x}^1 = dx^3 & | \mathbf{B}_1 (\mathbf{B}_2 - t\mathbf{A}_2) & (\mathbf{B}_3 - t\mathbf{A}_3) (\mathbf{B}_4 - t\mathbf{A}_4) & | \\ \mathbf{K}_{1x}^2 = -dx^2 dy & | \mathbf{A}_2 \mathbf{B}_2 & (\mathbf{B}_3 - t\mathbf{A}_3) (\mathbf{B}_4 - t\mathbf{A}_4) & | \\ \mathbf{K}_{1x}^3 = -dx^2 dy & | \mathbf{A}_3 (\mathbf{B}_2 - t\mathbf{A}_2) & \mathbf{B}_3 (\mathbf{B}_4 - t\mathbf{A}_4) & | \\ \mathbf{K}_{1x}^4 = -dx^2 dy & | \mathbf{A}_4 (\mathbf{B}_2 - t\mathbf{A}_2) & (\mathbf{B}_3 - t\mathbf{A}_3) \mathbf{B}_4 & | \end{array}$$

and the corresponding expressions for  $(\partial\zeta_1/\partial y)$  are

$$\begin{array}{llll} \mathbf{K}_{1y}^1 = & -dx^3 | \mathbf{A}_1 & (\mathbf{B}_2 - t\mathbf{A}_2) (\mathbf{B}_3 - t\mathbf{A}_3) & (\mathbf{B}_4 - t\mathbf{A}_4) | \\ \mathbf{K}_{1y}^2 = & dx^3 | \mathbf{A}_2 & \mathbf{B}_2 (\mathbf{B}_3 - t\mathbf{A}_3) & (\mathbf{B}_4 - t\mathbf{A}_4) | \\ \mathbf{K}_{1y}^3 = & dx^3 | \mathbf{A}_3 & (\mathbf{B}_2 - t\mathbf{A}_2) \mathbf{B}_3 & (\mathbf{B}_4 - t\mathbf{A}_4) | \\ \mathbf{K}_{1y}^4 = & dx^3 | \mathbf{A}_4 & (\mathbf{B}_2 - t\mathbf{A}_2) (\mathbf{B}_3 - t\mathbf{A}_3) & \mathbf{B}_4 | \end{array}$$

Obviously

$$\mathbf{K}_{1x}^2 = -t\mathbf{K}_{1y}^2 \quad \mathbf{K}_{1x}^3 = -t\mathbf{K}_{1y}^3 \quad \mathbf{K}_{1x}^4 = -t\mathbf{K}_{1y}^4. \quad (7)$$

Besides, expanding  $|\mathbf{K}|$  along the first line of the matrix results in

$$|\mathbf{K}| = dx\mathbf{K}_{1x}^1 + dy\mathbf{K}_{1y}^1,$$

so that along a characteristic curve  $\mathbf{K}_{1x}^1 = -t\mathbf{K}_{1y}^1$ . Corresponding equations are found for the other variables  $\zeta_j$   $j \geq 2$ :  $\mathbf{K}_{jx}^i = -t\mathbf{K}_{jy}^i$  if  $i \neq j$  whatever the value of  $|\mathbf{K}|$  and  $\mathbf{K}_{jx}^j = -t\mathbf{K}_{jy}^j$  if  $|\mathbf{K}| = 0$ . If the minors are not all null, this proves that the four (CE) derived from the boundedness of  $(\partial\zeta_k/\partial x)$  and their counterparts derived from the boundedness of  $(\partial\zeta_k/\partial y)$  are proportional so that only one set has to be studied. At this point, the case of the  $S$  curves and the one of the  $C^+$  and  $C^-$  curves shall be discussed separately.

#### 2.4. Number of independant (CE) along the $C^+$ and $C^-$

The abstract linear algebra point of view allows to calculate the number of independant (CE) in the specific case of the  $C^+$  and  $C^-$  curves. For  $dx \neq 0$ ,  $\mathbf{K}$  is easily found to be equivalent to

$$\left[ \begin{array}{cc} dx\mathbf{I} & 0 \\ \mathbf{A} & \mathbf{B} - t\mathbf{A} \end{array} \right] \quad \text{and then to} \quad \left[ \begin{array}{cc} dx\mathbf{I} & 0 \\ 0 & \mathbf{B} - t\mathbf{A} \end{array} \right]. \quad (8)$$

When the value  $t$  is the one corresponding to a  $C^+$  or a  $C^-$ , for both the adjoint and the direct problem, the rank of  $\mathbf{B} - t\mathbf{A}$  is known to be 3 from the eigenanalysis of Euler equations flux Jacobians. Using classical theorems for the rank of block diagonal matrices and the rank of equivalent matrices, the rank of  $\mathbf{K}$  is easily proven to be 7, one less than its size. In this case, the adjugate matrix is known to have rank one. This means that all (CE) (whose coefficients appear in the rows of the adjugate matrix) are proportional and reduced to only one independant equation. This result is very valuable as the corresponding explicit calculations from the algebraic expressions of the minors are very tedious. It has been used in §3.

### 2.5. Nullity of all minors along the $S$ curves

The  $4 \times 4$  determinant involved in the expression of  $\mathbf{K}_{1x}^1$  is

$$|\mathbf{B}_1 \quad (\mathbf{B}_2 - t\mathbf{A}_2) \quad (\mathbf{B}_3 - t\mathbf{A}_3) \quad (\mathbf{B}_4 - t\mathbf{A}_4)|. \quad (9)$$

Along a streamtrace  $t = dy/dx = v/u$  and  $(\mathbf{B} - t\mathbf{A})$  is a matrix of rank two. As all its minors of rank three are null, the determinant (9), calculated by expansion along the first column, appears to be zero. To get the same property for  $\mathbf{K}_{1x}^2, \mathbf{K}_{1x}^3$  and  $\mathbf{K}_{1x}^4$ , a straightforward rewriting is needed. For example, the determinant in  $\mathbf{K}_{1x}^2$  reads

$$|\mathbf{A}_2 \quad \mathbf{B}_2 \quad (\mathbf{B}_3 - t\mathbf{A}_3) \quad (\mathbf{B}_4 - t\mathbf{A}_4)| \text{ or possibly } |\mathbf{A}_2 \quad (\mathbf{B}_2 - t\mathbf{A}_2) \quad (\mathbf{B}_3 - t\mathbf{A}_3) \quad (\mathbf{B}_4 - t\mathbf{A}_4)|.$$

Under this last form, it is clearly null when the rank of  $(\mathbf{B} - t\mathbf{A})$  is two. Using the exact same arguments, it is possible to prove that all  $\mathbf{K}_{jx}^i$  and  $\mathbf{K}_{ix}^i$  are null when  $t = v/u$ .

Besides, we may change our point of view and consider (9) as a function of  $t$  for fixed  $W$ . This function is obviously a polynomial of maximum degree three and  $v/u$  is one of its roots. We hence expect  $(t - v/u)$  to be a factor of all  $\mathbf{K}_{jx}^i, \mathbf{K}_{jy}^i$  algebraic expressions. The explicit expressions of the coefficients for the (ACE) (see [27]) and (DCE) (see Appendix A) confirm this property.

Along the  $S$  curves,  $\mathbf{K}$  is found to have rank 6 thanks to the technique used in the previous subsection. As already stated, all  $\mathbf{K}_{jx}^i$  and  $\mathbf{K}_{jy}^i$  are zero and the adjugate matrix of  $\mathbf{K}$  is the null matrix. The derivation of the explicit (CE) along the trajectories then involves the multiplicity two of  $(-vdx + udy)$  and simplified  $\bar{\mathbf{K}}_{jx}^i, \bar{\mathbf{K}}_{jy}^i$  coefficients derived by removing  $(-vdx + udy)$  in the expressions of the corresponding  $\mathbf{K}_{jx}^i, \mathbf{K}_{jy}^i$ . The proportionality of the explicit (CE) derived from the boundedness of  $(\partial \zeta_k / \partial x)$  and  $(\partial \zeta_k / \partial y)$  is verified but is more easily presented based on the actual formulas of the (CE) – see §3 for the (DCE) and in [27] §2 for the (ACE).

## 3. Derivation of characteristic equations for 2D inviscid compressible flows using conservative variables.

### 3.1. Flow properties, sets of variables, resulting equations for the usual derivation of the characteristic equations

The classical derivations of the (DCE) use a set of Taylor expansions and mechanical equations for the variations of a set of primitive variables. These resulting equations are linear in the unknown derivatives of the primitive variables with non-linear functions of the state variables as coefficients. The variations are generally expressed in an orthonormal frame of reference  $(\vec{\xi}, \vec{\eta})$ . This frame is defined by its angle with respect to the one induced by the local flow motion, that we denote as  $(\vec{t}, \vec{n})$  with  $\phi$  the angle of  $\vec{t}$  w.r.t. the  $x$  axis. This approach leads to simpler expressions for the mechanical equations. Some orientations of the vector  $\vec{\xi}$  make the set of equations ill-posed:  $\vec{\xi} = \vec{t}$  for all flow regimes and  $\text{angle}(\vec{\xi}, \vec{t}) = \varepsilon \arcsin(1/M)$   $\varepsilon = \pm 1$ , if the flow is locally supersonic. The curves where at each point the tangent vector has one of these specific orientations with respect to the velocity are respectively the aforementioned streamtraces  $S$ ,  $C^+$  (for  $\varepsilon = 1$ ) and  $C^-$  (for  $\varepsilon = -1$ ). Along these curves equations with only  $\vec{\xi}$  derivatives are satisfied. These ODEs are the classical (DCE).

For a 2D flow of an ideal gas (§2.1), without any assumptions of constant stagnation enthalpy, or constant entropy or null vorticity: (a) the stagnation enthalpy and entropy are found to be constant along streamtraces; (b) one (DCE) is found along the  $C^+ C^-$  [3]. This (DCE), expressed in terms of variations of  $\phi$ ,  $\|\bar{U}\|, S$  and  $H$ , reads

$$\varepsilon d\phi - \sqrt{M^2 - 1} \frac{d\|\bar{U}\|}{\|\bar{U}\|} - \sqrt{M^2 - 1} \frac{TdS - dH}{\|\bar{U}\|^2} = 0, \quad (10)$$

where the Crocco equation can be used to rewrite the last term. If  $H$  is constant all over the fluid domain, the (DCE) also reads

$$\varepsilon d\phi - \frac{\sqrt{M^2 - 1}}{1 + \frac{\gamma - 1}{2} M^2} \frac{dM}{M} - \frac{\sqrt{M^2 - 1}}{\gamma r M^2} dS = 0. \quad (11)$$

If  $S$  is also constant, the flow is irrotational according to Crocco's theorem and the (DCE) reads

$$\varepsilon d\phi - \frac{\sqrt{M^2 - 1}}{1 + \frac{\gamma - 1}{2} M^2} \frac{dM}{M} = 0. \quad (12)$$

This equation can be integrated involving the Prandtl-Meyer function,

$$v(M) = \sqrt{\frac{\gamma+1}{\gamma-1}} \tan^{-1} \left( \sqrt{\frac{\gamma-1}{\gamma+1}} (M^2 - 1) \right) - \tan^{-1}(\sqrt{M^2 - 1}),$$

and the final algebraic equations resulting from the integration of (12) are

$$k^- = \phi + v(M) \text{ is constant along a } \mathcal{C}^- \quad k^+ = \phi - v(M) \text{ is constant along a } \mathcal{C}^+. \quad (13)$$

Other sets of primitive variables may be used to derive (10) and the resulting simplified equations [28, 4]. Also possible is the demonstration of these equations in a mapping of the plane rather than in the aforementioned frame of reference [28].

In case the flow is assumed to be irrotational from the beginning, a very fast demonstration is possible involving the velocity potential – see [29] or [2, 30, 31]. The governing nonlinear equation for a two-dimensional potential flow is:

$$\left(1 - \frac{u^2}{c^2}\right) \frac{\partial u}{\partial x} - \frac{2uv}{c^2} \frac{\partial u}{\partial y} + \left(1 - \frac{v^2}{c^2}\right) \frac{\partial v}{\partial y} = 0 \quad (14)$$

and of course

$$du = \frac{\partial u}{\partial x} dx + \frac{\partial u}{\partial y} dy \quad dv = \frac{\partial v}{\partial x} dx + \frac{\partial v}{\partial y} dy.$$

This results in a simple  $(3 \times 3)$  linear system for  $(\partial u/\partial x)$ ,  $(\partial v/\partial y)$  and  $(\partial u/\partial y)$  (that is equal to  $(\partial v/\partial x)$  for the potential flow) from which (12) and (13) are easily derived.

### 3.2. Derivation of the characteristic equations in conservative variables

The Cauchy problem aims at computing the derivatives  $(\partial W/\partial x)$   $(\partial W/\partial y)$  from the values of  $W$  at two neighboring points  $a$  and  $b$ . From the Euler equations and basic first order Taylor formulas, the equations of this problem read

$$\begin{bmatrix} dx & 0 & 0 & 0 & dy & 0 & 0 & 0 \\ 0 & dx & 0 & 0 & 0 & dy & 0 & 0 \\ 0 & 0 & dx & 0 & 0 & 0 & dy & 0 \\ 0 & 0 & 0 & dx & 0 & 0 & 0 & dy \\ & & & & & & & & A & & & & & & B \end{bmatrix} \begin{bmatrix} (\partial \rho/\partial x) \\ (\partial \rho u/\partial x) \\ (\partial \rho v/\partial x) \\ (\partial \rho E/\partial x) \\ (\partial \rho/\partial y) \\ (\partial \rho u/\partial y) \\ (\partial \rho v/\partial y) \\ (\partial \rho E/\partial y) \end{bmatrix} = \begin{bmatrix} d\rho \\ d\rho u \\ d\rho v \\ d\rho E \\ 0 \\ 0 \\ 0 \\ 0 \end{bmatrix} \quad (15)$$

with  $(dx, dy) = \vec{ab}$ ,  $(d\rho, d\rho u, d\rho v, d\rho E) = (\rho^b - \rho^a, \rho u^b - \rho u^a, \rho v^b - \rho v^a, \rho E^b - \rho E^a)$  and  $A, B$  the Euler flux Jacobian matrices. The determinant is easily calculated as

$$D = \begin{vmatrix} dxI & dyI \\ A & B \end{vmatrix} = \begin{vmatrix} dxI & 0 \\ A & B - (dy/dx)A \end{vmatrix} = dx^4 |B - (dy/dx)A| \quad (16)$$

Of course,  $D = |dxB - dyA| = |-dxB + dyA|$  and the problem is ill-posed along the  $S$ ,  $C^+$ ,  $C^-$  curves as recalled in §2.3. The fact that the Cauchy problem is ill-posed along these specific curves whereas  $(\partial W/\partial x)$  and  $(\partial W/\partial y)$  are actually defined and bounded, implies that not only the denominator in the Cramer formula applied to (15) is equal to zero but also the eight numerators corresponding to the unknowns  $(\partial \rho/\partial x)$ ,  $(\partial \rho u/\partial x)$ ,  $(\partial \rho v/\partial x)$ ,  $(\partial \rho E/\partial x)$   $(\partial \rho/\partial y)$ ,  $(\partial \rho u/\partial y)$ ,  $(\partial \rho v/\partial y)$ ,  $(\partial \rho E/\partial y)$  must be equal to zero. This is precisely the principle of the method of

characteristics that allows to derive ODEs along the characteristic curves.

The Euler flux Jacobian matrices in  $x$  and  $y$  direction,  $A$  and  $B$ , are equal to

$$A = \begin{bmatrix} 0 & 1 & 0 & 0 \\ \gamma_1 E_c - u^2 & (3-\gamma)u & -\gamma_1 v & \gamma_1 \\ -uv & v & u & 0 \\ (\gamma_1 E_c - H)u & H - \gamma_1 u^2 & -\gamma_1 uv & \gamma_1 u \end{bmatrix} \quad B = \begin{bmatrix} 0 & 0 & 1 & 0 \\ -uv & v & u & 0 \\ \gamma_1 E_c - v^2 & -\gamma_1 u & (3-\gamma)v & \gamma_1 \\ (\gamma_1 E_c - H)v & -\gamma_1 uv & H - \gamma_1 v^2 & \gamma_1 v \end{bmatrix}$$

(with  $\gamma_1 = \gamma - 1$ ) and the following notations are introduced:

$$t = \frac{dy}{dx}, \quad \kappa = ut - v.$$

The columns of Jacobian are denoted by  $A_1$  to  $A_4$  and  $B_1$  to  $B_4$  so that  $A = [A_1|A_2|A_3|A_4]$ ,  $B = [B_1|B_2|B_3|B_4]$ . The principle of the calculation of the ODE satisfied along the  $S$ ,  $C^+$  and  $C^-$  curves is recalled for variable  $(\partial\rho/\partial x)$  which boundedness requires that

$$\begin{vmatrix} d\rho & 0 & 0 & 0 & dy & 0 & 0 & 0 \\ d\rho u & dx & 0 & 0 & 0 & dy & 0 & 0 \\ d\rho v & 0 & dx & 0 & 0 & 0 & dy & 0 \\ d\rho E & 0 & 0 & dx & 0 & 0 & 0 & dy \\ | & | & | & | & | & | & | & | \\ 0 & A_2 & A_3 & A_4 & B_1 & B_2 & B_3 & B_4 \\ | & | & | & | & | & | & | & | \end{vmatrix} = 0. \quad (17)$$

The determinant is expanded along the first column with the notations of next equation:

$$K_{1x}^1 d\rho - K_{1x}^2 d\rho u + K_{1x}^3 d\rho v - K_{1x}^4 d\rho E = 0. \quad (18)$$

In this equation, for example

$$K_{1x}^4 = \begin{vmatrix} 0 & 0 & 0 & dy & 0 & 0 & 0 & 0 \\ dx & 0 & 0 & 0 & dy & 0 & 0 & 0 \\ 0 & dx & 0 & 0 & 0 & dy & 0 & 0 \\ | & | & | & | & | & | & | & | \\ A_2 & A_3 & A_4 & B_1 & B_2 & B_3 & B_4 & | \end{vmatrix} = \begin{vmatrix} 0 & 0 & 0 & dy & 0 & 0 & 0 & 0 \\ dx & 0 & 0 & 0 & 0 & 0 & 0 & 0 \\ 0 & dx & 0 & 0 & 0 & 0 & 0 & 0 \\ | & | & | & | & | & | & | & | \\ A_2 & A_3 & A_4 & B_1 & B_2 - tA_2 & B_3 - tA_3 & B_4 & | \end{vmatrix} \quad (19)$$

Finally

$$K_{1x}^4 = dx^2 dy | A_4 (B_2 - tA_2) (B_3 - tA_3) (B_4) | = dx^2 dy \kappa \gamma_1 (tv + u) \quad (20)$$

At this step, no assumption on the value of  $t$  with respect to the velocity vector  $(u, v)$ . The other terms of the differential form are equal to

$$K_{1x}^1 = -dx^3 \kappa (v \kappa^2 - \gamma_1 v (1+t^2)H + \gamma_1 (ut+v) E_c + 2 \gamma_1 t^2 v E_c) \quad (21)$$

$$K_{1x}^2 = -dx^2 dy \kappa (\gamma \kappa v + 2 \gamma_1 E_c) \quad (22)$$

$$K_{1x}^3 = dx^2 dy \kappa (-2t E_c + \gamma v (tv + u)) \quad (23)$$

The characteristic equation (18) can hence be rewritten as

$$\begin{aligned} & - dx^3 \kappa (v \kappa^2 - \gamma_1 v (1+t^2)H + \gamma_1 (ut+v) E_c + 2 \gamma_1 t^2 v E_c) d\rho \\ & + dx^2 dy \kappa (\gamma \kappa v + 2 \gamma_1 E_c) d\rho u + dx^2 dy \kappa (-2t E_c + \gamma v (tv + u)) d\rho v \\ & - dx^2 dy \kappa \gamma_1 (tv + u) d\rho E = 0 \end{aligned} \quad (24)$$

If  $dx \neq 0$  and  $\kappa \neq 0$ , this equation may be further simplified:

$$\begin{aligned} & - (v \kappa^2 - \gamma_1 v (1+t^2)H + \gamma_1 (ut+v)E_c + 2 \gamma_1 t^2 v E_c) d\rho \\ & + t (\gamma \kappa v + 2 \gamma_1 E_c) d\rho u + t (-2t E_c + \gamma v (tv + u)) d\rho v \\ & - t \gamma_1 (tv + u) d\rho E = 0 \end{aligned} \quad (25)$$

Of course, along the  $S$  curves,  $\kappa$  is null and the equation (25) seems to be only valid for the  $C^+$  and  $C^-$  curves. Actually as  $(-vdx + udy = \kappa dx)$  has a multiplicity of two in the determinant  $D$ , (25) is also needed for the existence of  $(\partial\rho/\partial x)$  along the  $S$  curves (see §3.3).

For the other seven partial derivatives, the expression of the coefficients of the (CE) are presented in the Appendix A. Besides, it is proven in §2 that,  $W_l$  being one of the four conservative variables, the equations for the boundedness of  $(\partial W_l/\partial x)$  and  $(\partial W_l/\partial y)$  along the characteristics are proportionnal by a  $-t$  factor. Therefore, only the counterpart of equation (25) for the existence of  $(\partial\rho u/\partial x)$ ,  $(\partial\rho v/\partial x)$  and  $(\partial\rho E/\partial x)$  are presented hereafter:

$$\begin{aligned}
& - \gamma_1 t E_c (-\gamma_1 H + (\gamma + 1) E_c) d\rho \\
& + (\gamma_1 (\gamma t u + \kappa) E_c + v^2 \kappa + \gamma_1 (v - \gamma_1 t u) H) d\rho u \\
& - t (u^2 \kappa + \gamma_1 (\kappa - \gamma v) E_c + \gamma_1 (\gamma_1 v - ut) H) d\rho v \\
& + t \gamma_1 (\gamma_1 H - (\gamma + 1) E_c) d\rho E = 0
\end{aligned} \tag{26}$$

$$\begin{aligned}
& + \gamma_1 E_c t^2 (\gamma_1 H - (\gamma + 1) E_c) d\rho \\
& - t (-v^2 \kappa - \gamma_1 \kappa E_c - \gamma \gamma_1 t u E_c + \gamma_1 (\gamma_1 t u - v) H) d\rho u \\
& + (-v^3 + 3t u v^2 - 2t^2 u^2 v + \gamma_1 ((2 - \gamma) t^2 v - \kappa) H + \gamma_1 (\gamma t^2 v + \kappa) E_c) d\rho v \\
& - t^2 \gamma_1 (-\gamma_1 H + (\gamma + 1) E_c) d\rho E = 0
\end{aligned} \tag{27}$$

$$\begin{aligned}
& - \gamma_1 t (u + tv) E_c (\gamma_1 E_c + (2 - \gamma) H) d\rho \\
& + t (\gamma_1 u^2 + v \kappa + \gamma_1 t u v) (\gamma_1 E_c + (2 - \gamma) H) d\rho u \\
& - t (u \kappa - \gamma_1 t v^2 - \gamma_1 u v) (\gamma_1 E_c + (2 - \gamma) H) d\rho v \\
& + (-v \kappa^2 - \gamma_1 ((1 + \gamma t^2) v + \gamma_1 t u) E_c + \gamma_1^2 t (u + tv) H - \gamma_1 \kappa H) d\rho E = 0
\end{aligned} \tag{28}$$

### 3.3. Ordinary differential equations along the streamtraces $S$

Along the trajectories,  $udy - vdx = 0$  is a zero of the denominator of Cramer's formulas with a multiplicity of two. The term  $\kappa dx = udy - vdx$  appears to be a factor of all  $K_{mx}^l$  and the expressions obtained by removing this term from  $K_{mx}^l$  is denoted by  $\bar{K}_{mx}^l$ . Obviously wherever the Cauchy problem is well-defined

$$\frac{\partial\rho}{\partial x} = \frac{\bar{K}_{1x}^1 d\rho - \bar{K}_{1x}^2 d\rho u + \bar{K}_{1x}^3 d\rho v - \bar{K}_{1x}^4 d\rho E}{(-v dx + u dy)(-v dx + u dy + c dl)(-v dx + u dy - c dl)}. \tag{29}$$

If the point  $a$  is fixed and the neighboring point  $b$  is moved closer and closer to  $S_a$ ,  $(-v dx + u dy) \rightarrow 0$  and the boundedness of  $(\partial\rho/\partial x)$  requires the numerator of (29) to be equal to zero:

$$\bar{K}_{1x}^1 d\rho - \bar{K}_{1x}^2 d\rho u + \bar{K}_{1x}^3 d\rho v - \bar{K}_{1x}^4 d\rho E = 0. \tag{30}$$

The expressions for the  $\bar{K}$  coefficients are much simpler than those of the  $K$  coefficients thanks to the nullity of  $\kappa$ . It can be verified by hand or by formal calculation that the (CE) expressing the boundedness of  $(\partial W_l/\partial x)$  and their counterparts for  $(\partial W_l/\partial y)$  are proportionnal by a  $-t$  factor. It is also possible to check that  $\bar{K}_{lx}^l = -t \bar{K}_{ly}^l$  and then use the continuity of the  $\bar{K}$  coefficients as functions of  $(W, dx, dy, \gamma)$  and the validity of  $\bar{K}_{mx}^l = -t \bar{K}_{my}^l$   $l <> m$  outside the variety  $udy - vdx = 0$ . We denote  $(\gamma_1 E_c + (2 - \gamma) H)$  as  $G$ ; The fully simplified differential forms then read

$$(2E_c - H) d\rho - u d\rho u - v d\rho v + d\rho E = 0 \tag{31}$$

$$((\gamma + 1) E_c - \gamma_1 H) (E_c d\rho + d\rho E) - (\gamma E_c + (2 - \gamma) H) (u d\rho u + v d\rho v) = 0 \tag{32}$$

$$-E_c G d\rho + u G d\rho u + v G d\rho v + (\gamma_1 H - \gamma E_c) d\rho E = 0, \tag{33}$$

where equation (32) is obtained twice, from the existence of the derivatives of both momentum components. The rank of the matrix was first calculated with Maple software and found unsurprisingly to be two. It can also be verified by hand calculation that  $E_c \times$  (31) minus (32) is exactly equation (33) and then, finally, that the  $d\rho$  and  $d\rho E$  columns in



{(31),(32)} are not linked.

Along the streamtrace  $S$ , the derivative of the total enthalpy,  $H$ , and the entropy,  $S$ , are expected to be null [29]. Before verifying that these properties are ensured by the (CE) found just before, the differential of  $p/\rho^\gamma$  times  $\rho^\gamma$  and the differential of  $H$  times  $\rho$  are calculated:

$$\rho^\gamma d(p/\rho^\gamma) = (2E_c - H) d\rho - u d\rho u - v d\rho v + d\rho E \quad (34)$$

$$\rho dH = (-\gamma E + 2(\gamma - 1)E_c) d\rho - \gamma_1 u d\rho u - \gamma_1 v d\rho v + \gamma d\rho E \quad (35)$$

Equation (31) is exactly the same as  $\rho^\gamma d(p/\rho^\gamma) = 0$ . This yields  $d(p/\rho^\gamma) = 0$  and obviously the derived (CE) contain the property of constant entropy along the streamtraces. Besides  $G \times$  (31) plus (33) yields, after simplification by a common factor,  $-Gd\rho + d\rho E = 0$ . Finally adding this equation to  $\gamma_1$  times equation (31), precisely yields  $\rho dH = 0$ , so that second expected property for Euler flows along the trajectories is contained in the derived (CE).

### 3.4. Ordinary differential equations along the $C^+ C^-$

The proportionality of all eight differential forms along the  $C^+$ ,  $C^-$  has been proven in §2.4. and equation (25) may be retained as the relevant (DCE). The factor of  $d\rho$  is quite complex in (25) but it admits a simpler form derived from the degree two equations satisfied by  $t^+$  and  $t^-$ : these curve slopes are defined as

$$t^\pm = \tan(\phi + \beta) \quad \text{with} \quad \tan \phi = \frac{v}{u} \quad \sin \beta = \pm \frac{1}{M}, \quad (36)$$

or alternatively by their explicit expressions [27]:

$$t^\pm = \frac{uv \pm c \sqrt{u^2 + v^2 - c^2}}{u^2 - c^2}. \quad (37)$$

They are the two roots of the following degree two equation [27]

$$\gamma_1 (1 + t^2) H = \gamma_1 (1 + t^2) E_c + (tu - v)^2, \quad (38)$$

which allows to simplify the expression of (25) along a  $C^+$  or a  $C^-$ . The final (DCE) reads

$$\gamma_1 E_c (u + tv) d\rho - (\gamma u (u + tv) - 2E_c) d\rho u - (\gamma v (u + tv) - 2E_c t) d\rho v + \gamma_1 (u + tv) d\rho E = 0 \quad (39)$$

with  $t = t^+$  for a  $C^+$  and by  $t = t^-$  for a  $C^-$ .

It has been first checked that this  $C^+$  (resp.  $C^-$ ) differential form is linked with  $\{dk^+, dH, dS\}$  (resp.  $\{dk^-, dH, dS\}$ ) consistently with equation (10). It proven in Appendix B that these (CE), expressed with different variables, are the same.

## 4. Assessment of the direct and adjoint characteristic equations for a nozzle flow

### 4.1. Supersonic nozzle configuration

The test case for the assessment of the (DCE) and (ACE) is a supersonic nozzle designed for an aircraft flying at Mach 1.6. The geometry was designed in the framework of the SENECA EU project [32]. The nozzle is a classical convergent-divergent duct. At the subsonic injection plane, the stagnation conditions are fixed and the ratio of the farfield flow static pressure (resp. temperature) to the total pressure (resp. total temperature) at the inlet are  $p_{i_{inl}}/p_{i_\infty} = 1.605$  and  $T_{i_{inl}}/T_{i_\infty} = 1.606$ . As an inviscid flow is calculated, these two conditions and the farfield-Mach number fully define the flow.

The original geometry was designed for a circular axisymmetric engine and the nozzle contour in the symmetry plane was simply extracted to define the 2D geometry. Consequently the mass flow rates are different. Due the different laws of areas along the  $x$  coordinate (the inlet and main flow direction), the flows are also different along the midline of the nozzle. Nevertheless, the Mach number distribution along this line are similar with  $M = 1$  at the throat and

$M \simeq 2.1$  at the exit.

The functional output of interest is the thrust  $T$ ,

$$T = \int_{\Gamma_w} (p - p_\infty) ds_x + \int_{\Gamma_{inl}} (\rho u^2 + p) ds_x, \quad (40)$$

where  $\Gamma_w$  is the internal wall of the nozzle,  $\Gamma_{inl}$  the injection section, and  $s_x$  the  $x$ -component of the surface vector (oriented towards the outside of the fluid domain).

The nozzle and the fluid domain are presented in figure 1 as well as the Mach-number distribution and the  $S$ ,  $C^+$  and  $C^-$  curves selected for the (CE) assessment. A structured 8-block mesh with 320000 cells discretizes the fluid domain. The flow simulations are run with the *elsA* code [33] using the Jameson-Schmidt-Turkel (JST) scheme [34]. The adjoint calculation for the thrust is run with the discrete adjoint module of the *elsA* code [35] which is used for both research [36, 37, 12, 38] and application [39, 40, 41] purposes. In [38], it is proven that the discrete adjoint of the (JST) scheme on a structured mesh is dual consistent for Euler flows but in the cells next to those adjacent to a boundary. This adjoint consistency property inside the fluid domain is very valuable to numerically assess continuous adjoint properties. The change in the Jacobian to get the dual consistency in the vicinity of the physical boundaries is complex to implement in an industrial code. In this study, it is not used and slight oscillations of the adjoint field are observed near the boundaries. For the sake of simplicity, considering the mesh density, the points inside the first two cells in the vicinity of a boundary are removed from the extracted characteristic curves. The first component of the adjoint field is presented in figure 3. The exact adjoint of the thrust is expected to be zero downstream the backward  $C^+$  characteristic (and corresponding  $C^-$  in the symmetric non-plotted domain) emanating from the rear of the nozzle, as no perturbation downstream these lines can affect the flow on the support of  $T$  (We recall that the velocity is supersonic in the divergent part of the nozzle). This property is well satisfied by the discrete adjoint.

A series of recent publications have studied the properties the Euler lift- and drag-adjoint fields, in particular in the vicinity of the wall [42, 43, 44, 45, 38]. One of the remarkable properties of these fields when associated to a wall-pressure integral is the proportionality of  $\psi_1$  and  $\psi_4$  by a factor  $H$  [46] which is numerically very well satisfied [38]. In addition to the validation of the paper results, we take the opportunity provided by the specific function of interest (40) (that does not only depend on the static pressure), to plot together  $\psi_1$  and  $H\psi_4$  – see figure 3. The two quantities seem similar and further studies may be devoted to the conditions on the output functional of interest for which  $\psi_1 = H\psi_4$  should be observed.

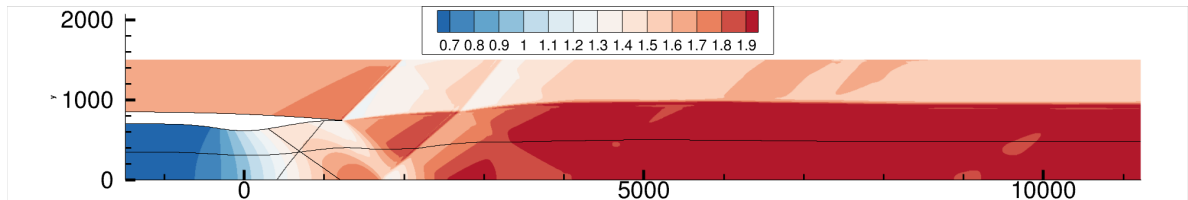


Figure 1: SENECA nozzle. Iso-Mach number lines. Selected  $S$ ,  $C^+$  and  $C^-$  for the validation of the (DCE) and (ACE)

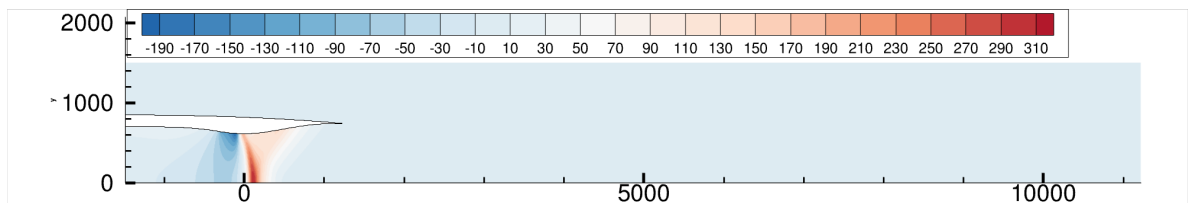


Figure 2: SENECA nozzle. Iso lines of the discrete adjoint of the thrust, component  $\psi_1$  (dual of the mass-flow residual)

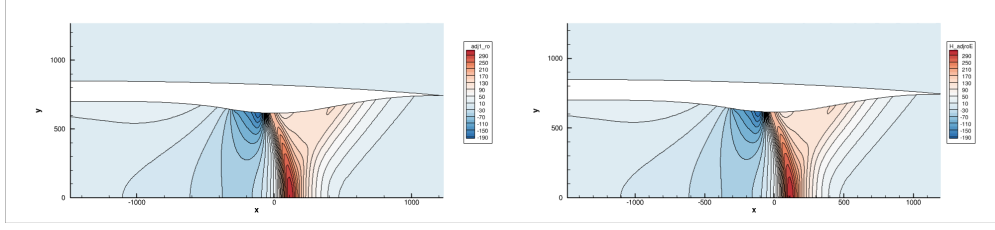


Figure 3: SENECA nozzle. Iso- $\psi_1$  (left) and iso- $(H \times \psi_4)$  with same levels

#### 4.2. Assessment of the (CDE)

The numerical assessment method consists in integrating the (CDE) along the characteristic curves for the aforementioned fine mesh flow. More precisely, for the  $C^+$  and  $C^-$ , the following integrals are calculated

$$\begin{aligned} \Xi C^+ &= \int_{\mathcal{C}^+} \left( \gamma E_c(u+vt^+) \frac{d\rho}{ds} - (\gamma u(u+vt^+) - 2E_c) \frac{d\rho u}{ds} - (\gamma v(u+vt^+) - 2E_c t^+) \frac{d\rho v}{ds} + \gamma_1(u+vt^+) \frac{d\rho E}{ds} \right) ds \\ \Xi C^- &= \int_{\mathcal{C}^-} \left( \gamma E_c(u+vt^-) \frac{d\rho}{ds} - (\gamma u(u+vt^-) - 2E_c) \frac{d\rho u}{ds} - (\gamma v(u+vt^-) - 2E_c t^-) \frac{d\rho v}{ds} + \gamma_1(u+vt^-) \frac{d\rho E}{ds} \right) ds, \end{aligned}$$

with  $s$  the curvilinear abscissa along the characteristic curve. The subparts of  $\Xi C^+$  and  $\Xi C^-$  are also calculated to avoid any error in scale when discussing close to zero numerical values. For  $\Xi C^+$ , for example,

$$\begin{aligned} \Xi C_1^+ &= \int_{\mathcal{C}^+} \left( \gamma E_c(u+vt^+) \frac{d\rho}{ds} \right) ds & \Xi C_2^+ &= - \int_{\mathcal{C}^+} \left( (\gamma u(u+vt^+) - 2E_c) \frac{d\rho u}{ds} \right) ds \\ \Xi C_3^+ &= - \int_{\mathcal{C}^+} \left( (\gamma v(u+vt^+) - 2E_c t^+) \frac{d\rho v}{ds} \right) ds & \Xi C_4^+ &= \int_{\mathcal{C}^+} \left( \gamma_1(u+vt^+) \frac{d\rho E}{ds} \right) ds. \end{aligned}$$

Of course, the  $\Xi C^+ = \Xi C_1^+ + \Xi C_2^+ + \Xi C_3^+ + \Xi C_4^+$  (resp.  $\Xi C^- = \Xi C_1^- + \Xi C_2^- + \Xi C_3^- + \Xi C_4^-$ ) sum is expected to be much smaller than its subparts. The integration is performed in the information propagation direction (increasing  $x$ ) along the selected  $C^+$  and the selected  $C^-$  presented in figure 1. Almost null values of  $\Xi C^+$  and  $\Xi C^-$  are indeed observed – see figure 4. Equivalent successful verifications have been performed to assess the validity of (31) and

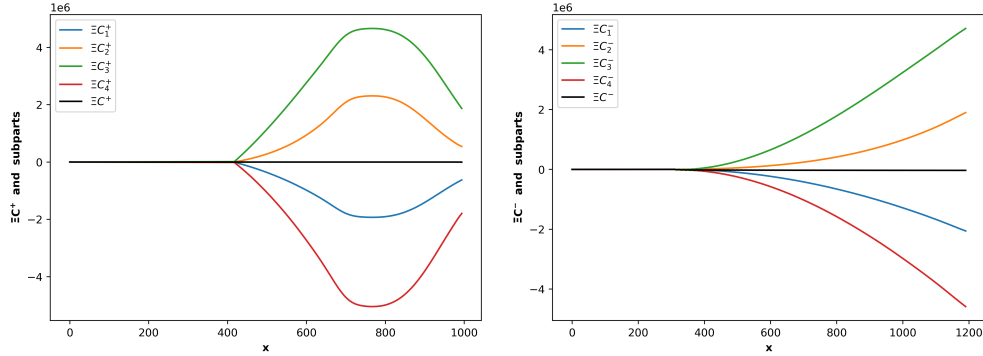


Figure 4: Numerical assessment of (DCE) (39).  $\Xi C^+$  (left),  $\Xi C^-$  (right) and their subparts integrated along the selected  $C^+ C^-$ . Method of verification: the black curve should ideally coincide with the  $x$  axis.

(32). They are not presented here for the sake of brevity. These two streamtraces (DCE) are equivalent to  $dS = 0$  and  $dH = 0$  as discussed in §3.3. As a complementary verification, the relative variation of  $H$  (all over the streamtrace) and  $S$  (up to the first shockwave) are calculated. Relative errors of  $3e^{-6}$  and  $4e^{-6}$  are found.

#### 4.3. Assessment of the (ACE) for the thrust-adjoint

For the thrust-adjoint, the assessment method is the same except that the (ACE) are integrated in the forward sense for the adjoint, that is, from the support of the functional output backwards w.r.t. the direction of the flow

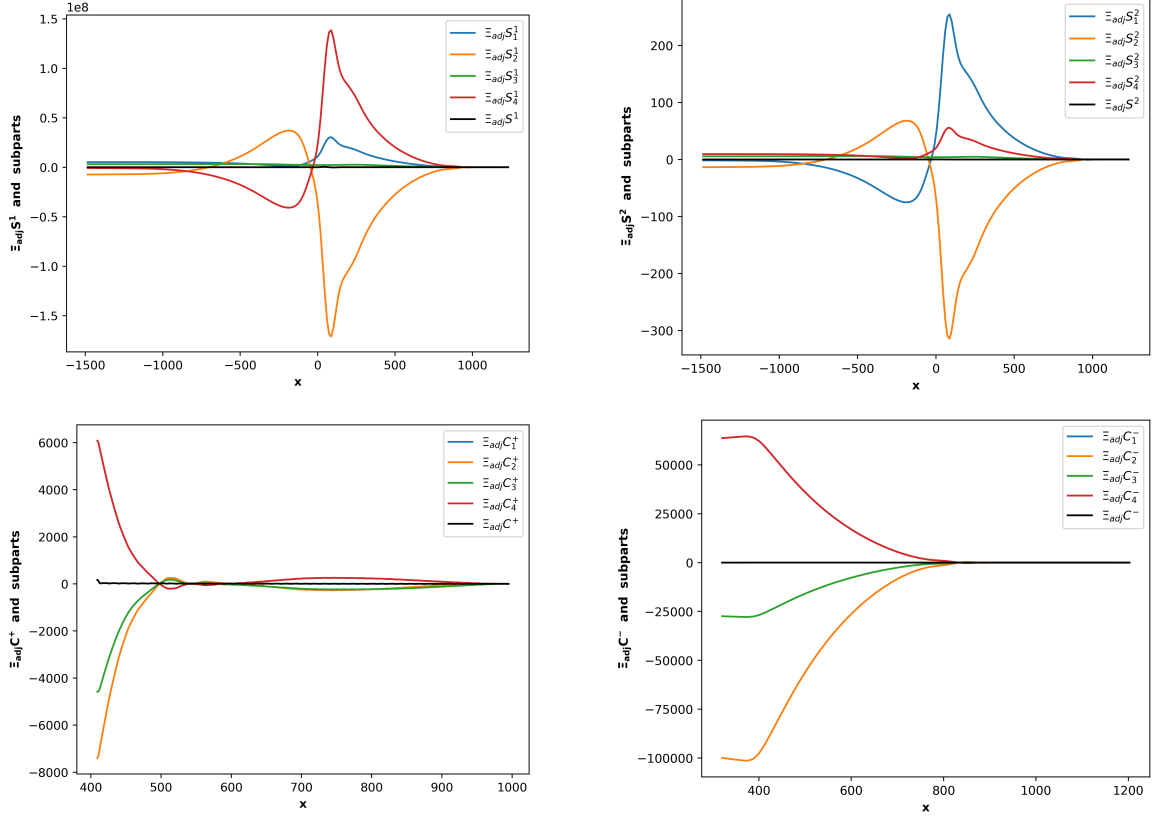


Figure 5: Numerical assessment of the (ACE)[27].  $\Xi_{adj}S^1$  (upper left),  $\Xi_{adj}S^2$  (upper right),  $\Xi_{adj}C^+$  (bottom left),  $\Xi_{adj}C^-$  (bottom right) and their subparts integrated along the selected  $S$ ,  $C^+$  and  $C^-$ . Method of verification: the black curve should ideally coincide with the  $x$  axis.

information propagation. The integrals to evaluate (as well as their subparts) from the discrete flow and thrust-adjoint fields are[27]:

$$\Xi_{adj}S^1 = \int_{\mathcal{S}} \left( E_c \frac{d\psi_1}{ds} + H(u \frac{d\psi_2}{ds} + v \frac{d\psi_3}{ds}) + H^2 \frac{d\psi_4}{ds} \right) ds \quad (41)$$

$$\Xi_{adj}S^2 = \int_{\mathcal{S}} \left( \frac{d\psi_1}{ds} + u \frac{d\psi_2}{ds} + v \frac{d\psi_3}{ds} + E_c \frac{d\psi_4}{ds} \right) ds \quad (42)$$

$$\Xi_{adj}C^+ = \int_{\mathcal{C}^+} \left( (u + vt^+) \frac{d\psi_1}{ds} + (u^2 + v^2) \left( \frac{d\psi_2}{ds} + t^+ \frac{d\psi_3}{ds} \right) + H(u + vt^+) \frac{d\psi_4}{ds} \right) ds \quad (43)$$

$$\Xi_{adj}C^- = \int_{\mathcal{C}^-} \left( (u + vt^-) \frac{d\psi_1}{ds} + (u^2 + v^2) \left( \frac{d\psi_2}{ds} + t^- \frac{d\psi_3}{ds} \right) + H(u + vt^-) \frac{d\psi_4}{ds} \right) ds. \quad (44)$$

As in §4.2, the (CE) are numerically assessed by checking that  $\Xi_{adj}S^1$ ,  $\Xi_{adj}S^2$ ,  $\Xi_{adj}C^+$  and  $\Xi_{adj}C^-$  are much smaller than their subterms all along the characteristic curves. This property is actually well satisfied as can be seen in figure 5.

## 5. Conclusion

A few years ago, several authors had the intuition that the lift- and drag-adjoint fields of the supersonic areas of 2D inviscid flows were linked to the characteristic curves [20, 47]. This was recently confirmed by the extension of the theory of characteristics to the continuous adjoint equations of 2D Euler flows [27]. The application section of this paper provides a second numerical assessment of these equations.

Besides, the derivation of the (ACE) in [27] required the analytical calculation of the minors of a  $8 \times 8$  Cauchy problem matrix. The counterpart demonstration had never been applied for the search of the (CE) of the flow (the analysis of a set of physical equations, in a frame attached to the local velocity, being the classical way to proceed). It appears that the search of the (DCE) in conservative variables in the original frame of reference is feasible and not too complex. The corresponding derivation is greatly simplified by algebraic properties, presented in this contribution, which are shared by the linear systems of the Cauchy problem involved in both, the (DCE) and (ACE) search.

## Supplementary materials

Three Python files checking the formulas of  $K_{mx}^l$ ,  $K_{my}^l$ ,  $\bar{K}_{mx}^l$ ,  $\bar{K}_{my}^l$ .  
Two Maple files checking the rank of the differential forms along  $S$  and  $C^+$  curves.

## Funding

The nozzle considered in §4 was designed in the framework of the SENECA project that is funded by the European Union's Horizon 2020 research and innovation programme under grant agreement No. 101006742, project SENECA ((LTO) Noise and Emissions of Supersonic Aircraft). This work was partially supported by the SONICE project, granted by the French Directorate General for Civil Aviation (DGAC).

## Acknowledgements

elsA V5.0 used in §4 is ONERA-Safran property. The authors warmly thank Sébastien Heib, Sana Amri, Sébastien Bourasseau, Thomas Hennion and Antoine Dumont for many fruitful discussions.

## Authors contribution

Investigation, K.Ancourt, J.Peter ; Software, J.Peter ; Validation, K.Ancourt, O.Atinault ; Writing, J.Peter, K.Ancourt, O.Atinault ; Formal Analysis, K.Ancourt.

## Appendix A

- The  $K_{2x}^l$  coefficients are expressed below

$$\begin{aligned} K_{2x}^1 &= -dx^3 \gamma_1 t E_c \kappa (\gamma_1 H - (\gamma + 1)E_c) \\ K_{2x}^2 &= dx^3 \kappa (\gamma_1^2 t u E_c + \gamma_1 E_c \kappa + v^2 \kappa + \gamma_1 H v - \gamma_1^2 H t u + \gamma_1 t u E_c) \\ K_{2x}^3 &= -dx^3 t \kappa (-u^2 \kappa + \gamma_1 ((\gamma + 1) v - t u) E_c + \gamma_1 H (t u - \gamma_1 v)) \\ K_{2x}^4 &= -dx^3 \gamma_1 t \kappa (-\gamma_1 H + (\gamma + 1)E_c) \end{aligned}$$

- The  $K_{3x}^l$  coefficients are expressed below

$$\begin{aligned} K_{3x}^1 &= -dx^3 \gamma_1 t^2 E_c \kappa (-\gamma_1 H + (\gamma + 1)E_c) \\ K_{3x}^2 &= -dx^3 t \kappa (\gamma_1 ((\gamma + 1) t u - v) E_c + v^2 \kappa + \gamma_1 H (v - \gamma_1 t u)) \\ K_{3x}^3 &= dx^3 \kappa (-v^3 + 3 t u v^2 - \gamma_1 H \kappa - 2 t^2 u^2 v + \gamma_1^2 t^2 v E_c + \gamma_1 H t^2 v \\ &\quad - \gamma_1^2 H t^2 v + \gamma_1 t^2 v E_c + \gamma_1 E_c \kappa) \\ K_{3x}^4 &= -dx^3 \gamma_1 t^2 \kappa (\gamma_1 H - (\gamma + 1) E_c) \end{aligned}$$

- The  $K_{4x}^l$  coefficients are expressed below

$$\begin{aligned}
K_{4x}^1 &= dx^3 \gamma_1 t E_c \kappa (u + t v) (\gamma_1 E_c + (2 - \gamma) H) \\
K_{4x}^2 &= dx^3 t \kappa (2 \gamma_1 E_c + \gamma \kappa v) (\gamma_1 E_c + (2 - \gamma) H) \\
K_{4x}^3 &= -dx^3 t \kappa (-u \kappa + \gamma_1 t v^2 + \gamma_1 u v) (\gamma_1 E_c + (2 - \gamma) H) \\
K_{4x}^4 &= dx^3 \kappa (-\gamma_1 H \kappa - \gamma_1 v E_c - v \kappa^2 - \gamma_1^2 t u E_c - \gamma_1 t^2 v E_c \\
&\quad - \gamma_1^2 t^2 v E_c + \gamma_1^2 H t u + \gamma_1^2 H t^2 v)
\end{aligned}$$

- The  $K_{1y}^l$  coefficients are expressed below

$$\begin{aligned}
K_{1y}^1 &= dx^3 \kappa (u \kappa^2 + 2 \gamma_1 u E_c + \gamma_1 t v E_c + \gamma_1 t^2 u E_c - \gamma_1 H (1 + t^2) u) \\
K_{1y}^2 &= dx^3 \kappa (\gamma \kappa v + 2 \gamma_1 E_c) \\
K_{1y}^3 &= dx^3 \kappa (-\gamma_1 v (t v + u) + \kappa u) \\
K_{1y}^4 &= -dx^3 \gamma_1 \kappa (t v + u)
\end{aligned}$$

- The  $K_{2y}^l$  coefficients are expressed below

$$\begin{aligned}
K_{2y}^1 &= dx^3 \gamma_1 E_c \kappa (\gamma_1 H - (\gamma + 1) E_c) \\
K_{2y}^2 &= dx^3 \kappa (\gamma_1 E_c (t \kappa - \gamma u) + t^2 u^3 + 2 u v^2 - 3 t u^2 v + \gamma_1 H ((\gamma - 2) u - t \kappa)) \\
K_{2y}^3 &= dx^3 \kappa (-u^2 \kappa + \gamma_1 ((\gamma + 1) v - t u) E_c + \gamma_1 H (t u - \gamma_1 v)) \\
K_{2y}^4 &= dx^3 \gamma_1 \kappa (-\gamma_1 H + (\gamma + 1) E_c)
\end{aligned}$$

- The  $K_{3y}^l$  coefficients are expressed below

$$\begin{aligned}
K_{3y}^1 &= dx^3 \gamma_1 E_c \kappa t (-\gamma_1 H + (\gamma + 1) E_c) \\
K_{3y}^2 &= dx^3 \kappa (\gamma_1 ((\gamma + 1) t u - v) E_c + v^2 \kappa + \gamma_1 H (v - \gamma_1 t u)) \\
K_{3y}^3 &= dx^3 \kappa t (\gamma_1 H (\gamma_1 v - t u) - 2 \gamma_1 v E_c - \gamma_1^2 v E_c + u^2 \kappa + \gamma_1 t u E_c) \\
K_{3y}^4 &= dx^3 \gamma_1 \kappa t (\gamma_1 H - (\gamma + 1) E_c)
\end{aligned}$$

- The  $K_{4y}^l$  coefficients are expressed below

$$\begin{aligned}
K_{4y}^1 &= -dx^3 \gamma_1 E_c \kappa (u + t v) (\gamma_1 E_c + (2 - \gamma) H) \\
K_{4y}^2 &= -dx^3 \kappa (2 \gamma_1 E_c + \gamma \kappa v) (\gamma_1 E_c + (2 - \gamma) H) \\
K_{4y}^3 &= dx^3 \kappa (-u \kappa + \gamma_1 t v^2 + \gamma_1 u v) (\gamma_1 E_c + (2 - \gamma) H) \\
K_{4y}^4 &= dx^3 \kappa (u \kappa^2 + \gamma \gamma_1 u E_c + \gamma_1 t^2 u E_c + \gamma_1^2 t v E_c - \gamma_1^2 H u - \gamma_1^2 H t v \\
&\quad - \gamma_1 H t^2 u + \gamma_1 H t v)
\end{aligned}$$

## Appendix B

Let us prove the equivalence between (10) and (39) in case of a  $C^+$ . Equation (10) reads

$$d\phi - \sqrt{M^2 - 1} \frac{d\|\bar{U}\|}{\|\bar{U}\|} - \sqrt{M^2 - 1} \frac{T dS - dH}{\|\bar{U}\|^2} = 0,$$

with

$$\phi = \arctan\left(\frac{\rho v}{\rho u}\right) \quad \text{and} \quad T = \frac{p}{\rho r} \quad \text{so that} \quad T dS = \frac{p}{\rho \gamma_1} d\left(\ln\left(\frac{p}{\rho^\gamma}\right)\right) = \frac{p}{\rho \gamma_1} \left(\frac{dp}{p} - \gamma \frac{d\rho}{\rho}\right).$$

Moving from differentiation w.r.t. primitive variables to differentiation w.r.t. conservative variables yields

$$\gamma_1 E_c \sqrt{M^2 - 1} d\rho - (v + \gamma_1 u \sqrt{M^2 - 1}) d\rho u + (u - \gamma_1 v \sqrt{M^2 - 1}) d\rho v + \gamma_1 \sqrt{M^2 - 1} d\rho E = 0. \quad (45)$$

Besides, equation (39) reads

$$\gamma_1 E_c (u + t^+ v) d\rho - (\gamma u (u + t^+ v) - 2E_c) d\rho u - (\gamma v (u + t^+ v) - 2E_c t^+) d\rho v + \gamma_1 (u + t^+ v) d\rho E = 0$$

It appears that the coefficient of the last two equations are proportional:

$$\frac{\gamma_1 E_c (u + t^+ v)}{\gamma_1 E_c \sqrt{M^2 - 1}} = \frac{-(\gamma u (u + t^+ v) - 2E_c)}{-(v + \gamma_1 u \sqrt{M^2 - 1})} = \frac{-(\gamma v (u + t^+ v) - 2E_c t^+)}{(u - \gamma_1 v \sqrt{M^2 - 1})} = \frac{\gamma_1 (u + t^+ v)}{\gamma_1 \sqrt{M^2 - 1}} = (u + t^+ v) \tan \beta. \quad (46)$$

## Bibliography

### References

- [1] Ferri, A. Application of the method of characteristics to supersonic rotational flow. TR 841, NASA, (1946).
- [2] Shapiro, A. *The Dynamics and Thermodynamics of Compressible Fluid Flow*. The Ronald Press Company, (1954).
- [3] Bonnet, A. and Luneau, J. *Aérodynamique. Théories de la dynamique des fluides*. Cepadues, (1989).
- [4] Détery, J. *Traité d'aérodynamique compressible. Volume 3*. Collection mécanique des fluides. Lavoisier – Hermès Science, (2008).
- [5] Jameson, A. Aerodynamic design via control theory. *Journal of Scientific Computing* **3**(3), 233–260 (1988).
- [6] Brezillon, J. and Gauger, N. 2D and 3D aerodynamic shape optimization using the adjoint approach. *Aerospace Science and Technology Journal* **8**(8), 715–727 (2004).
- [7] Brezillon, T. and Dwight, R. Discrete adjoint of the navier-sotkes equations for aerodynamic shape optimization. In *EUROGEN 2005, Munich*, (2005).
- [8] Peter, J. and Dwight, R. Numerical sensitivity analysis for aerodynamic optimization: a survey of approaches. *Computers and Fluids* **39**, 373–391 (2010).
- [9] Schmidt, S., Ilic, C., Schultz, V., and Gauger, N. Three dimensional large scale aerodynamic shape optimization based on shape calculus. *AIAA Journal* **51**(11), 2615–2627 (2013).
- [10] Venditti, D. and Darmofal, D. Grid adaptation for functional outputs: Application to two-dimensional inviscid flows. *Journal of Computational Physics* **176**, 40–69 (2002).
- [11] Dwight, R. Heuristic *a posteriori* estimation of error due to dissipation in finite volume schemes and application to mesh adaptation. *Journal of Computational Physics* **227**, 2845–2863 (2008).
- [12] Todarello, G., Vonck, F., Bourasseau, S., Peter, J., and Désidéri, J.-A. Finite-volume goal-oriented mesh-adaptation using functional derivative with respect to nodal coordinates. *Journal of Computational Physics* **313**, 799–819 (2016).
- [13] Giles, M., Duta, M., and Müller, J.-D. Adjoint code developments using the exact discrete approach. In *AIAA Paper Series, Paper 2001-2596*. (2001).
- [14] Giles, M., Duta, M., Müller, J.-D., and Pierce, N. Algorithm developments for discrete adjoint methods. *AIAA Journal* **41**(2) (2003).
- [15] Economon, T., Alonso, J., Albring, T., and Gauger, N. Adjoint formulation investigations of benchmark aerodynamic design cases in SU2. In *AIAA Paper Series, Paper 2017-4363*. (2017).
- [16] Sagebaum, M., Albring, T., and Gauger, N. High-performance derivative computations using codipack. *ACM Transactions on Mathematical Software* **45**(4), 1–26 (2019).
- [17] Pinel, X. and Montagnac, M. Block Krylov methods to solve adjoint problems in aerodynamic design optimization. *AIAA Journal* **51**(9), 2183–2189 (2013).
- [18] Xu, S., Radford, D., Meyer, M., and Müller, J.-D. Stabilisation of discrete steady adjoint solvers. *Journal of Computational Physics* **299**, 175–195 (2015).
- [19] Lions, J. L. *Contrôle optimal de systèmes gouvernés par des équations aux dérivées partielles*. Etudes mathématiques. Paris: Dunod, Gauthier-Villars, (1968).
- [20] Sartor, F., Mettot, C., and Sipp, D. Stability, receptivity, and sensitivity analyses of buffeting transonic flow over a profile. *AIAA Journal* **53**(7), 1980–1993 (2015).
- [21] Laurenceau, J. *Surfaces de réponses par Krigeage pour l'optimisation de formes*. PhD thesis, Institut National Polytechnique de Toulouse, (2008).
- [22] de Baar, J., Scholcz, T., and Dwight, R. Technical note: Exploiting adjoint derivatives in high-dimensional metamodels. *AIAA Journal* **53**(5), 1391–1395 (2015).
- [23] Sipp, D., Marquet, O., Meliga, P., and Barbagallo, A. Dynamics and control of global instabilities in open-flows: A linearized approach. *Applied Mechanics Reviews* **63**(3) 04 (2010).
- [24] Luchini, P. and Bottaro, A. Adjoint equations in stability analysis. *Annual Review of Fluid Mechanics* **46**(1), 493–517 (2014).
- [25] Parish, E. and Duraisamy, K. A paradigm for data-driven predictive modeling using field inversion and machine learning. *Journal of Computational Physics* **305**, 758–774 (2016).
- [26] Talagrand, O. and Courtier, P. Variational assimilation of meteorological observations with the adjoint vorticity equation. I: Theory. *Q. J. R. Meteorol. Soc.* **113**(478), 1311–1328 (1987).

- [27] Peter, J. and Désidéri, J.-A. Ordinary differential equations for the adjoint euler equations. *Physics of Fluids* **34** 086113, 799–819 (2022).
- [28] Meyer, R. and Goldstein, S. The method of characteristics for problems of compressible flow involving two independant variables: Part i. the general theory. *The Quarterly Journal of Mechanics and Applied Mathematics* **1**(1), 196–219 (1948).
- [29] Anderson, J. *Modern Compressible Flow (third edition)*. McGraw-Hill series in Aeronautical and Aerospace Engineering, (2003).
- [30] Liepmann, H.W. and Roshko, A. *Elements of Gasdynamics*. Dover Publications, (1956).
- [31] Grossman, B. Fundamental concepts of real gasdynamics. virginia polytechnic institute and state university, January (2000).
- [32] Mourouzidis, M. Preliminary design of next generation mach 1.6 supersonic business jets to investigate landing and take-off (lto) noise and emissions. In *12th EASN conference on Innovation and Space for opening New Horizons, Barcelone*, (2022).
- [33] Cambier, L., Heib, S., and Plot, S. The elsA CFD software: input from research and feedback from industry. *Mechanics & Industry* **14**(3), 159–174 (2013).
- [34] Jameson, A., Schmidt, W., and Turkel, E. Numerical solutions of the Euler equations by finite volume methods using Runge-Kutta time-stepping schemes. In *AIAA Paper Series, Paper 1981-1259*. (1981).
- [35] Peter, J., Renac, F., Dumont, A., and Méheut, M. Discrete adjoint method for shape optimization and mesh adaptation in the *elsA* code. status and challenges. In *50th 3AF Symposium on Applied Aerodynamics, Toulouse*, (2015).
- [36] Peter, J., Drullion, F., and Pham, C.-T. Contribution to discrete implicit gradient and discrete adjoint method for aerodynamic shape optimization. In *ECCOMAS conference, Jyväskylä*, July (2004).
- [37] Peter, J., Nguyen-Dinh, M., and Trontin, P. Goal-oriented mesh adaptation using total derivative of aerodynamic functions with respect to mesh coordinates – with application to Euler flows. *Computers and Fluids* **66**, 194–214 (2012).
- [38] Peter, J., Renac, F., and Labbé, C. Analysis of finite-volume discrete adjoint fields for two-dimensional compressible Euler flows. *Journal of Computational Physics* **449**, 110811 (2022).
- [39] Carrier, G., Destarac, D., Dumont, A., Méheut, M., Salah el Din, I., Peter, J., Ben Khelil, S., Brezillon, J., and Pestana, M. Gradient-based optimization with the *elsA* software. In *AIAA Paper Series, Paper 2014-0568*. (2014).
- [40] Méheut, M., Destarac, D., Ben Khelil, S., Carrier, G., Dumont, A., and Peter, J. Gradient-based single- and multi-point optimization with the *elsA* software. In *AIAA Paper Series, Paper 2015-0263*. (2015).
- [41] Méheut, M., Carrier, G., Dumont, A., and Peter, J. Gradient-based optimization of crm wing-alone and wing-body-tail configurations by rans adjoint technique. In *AIAA Paper Series, Paper 2016-1293*. (2016).
- [42] Lozano, C. On mesh sensitivities and boundary formulas for discrete adjoint-based gradients in inviscid aerodynamic shape optimization. *Journal of Computational Physics* **346**, 403–436 (2017).
- [43] Lozano, C. Singular and discontinuous solutions of the adjoint Euler equations. *AIAA Journal* **56**(11), 4437–4451 (2018).
- [44] Lozano, C. Watch your adjoints! lack of mesh convergence in inviscid adjoint solutions. *AIAA Journal* **57**(9), 3991–4006 (2019).
- [45] Peter, J. Contributions to discrete adjoint method in aerodynamics for shape optimization and goal-oriented mesh adaptation. University of Nantes. Mémoire pour Habilitation à Diriger des Recherches, (2020).
- [46] Giles, M. and Pierce, N. Analytic adjoint solutions for the quasi-one-dimensional Euler equations. *Journal of Fluid Mechanics* **426**, 327–345 (2001).
- [47] Lozano, C. On the properties of the solutions of the 2D adjoint Euler equations. In *EUROGEN 2017, Madrid*, (2017).